Prediction of the rate of decline in FEV_1 in smokers using quantitative computed tomography

R Yuan,[1,2] J C Hogg,[1,3] P D Paré,[1,4] D D Sin,[1,4] J C Wong,[1] Y Nakano,[5] A M McWilliams,[4,6] S Lam,[4,6] H O Coxson[1,2]

► Additional details are published online only at http://thorax.bmj.com/content/vol64/issue11

[1] University of British Columbia James Hogg iCAPTURE Centre for Cardiovascular and Pulmonary Research and the Providence Heart + Lung Institute, St Paul's Hospital, Vancouver, British Columbia, Canada; [2] Department of Radiology, Vancouver General Hospital, University of British Columbia, Vancouver, British Columbia, Canada; [3] Department of Pathology and Laboratory Medicine, University of British Columbia, Vancouver, British Columbia, Canada; [4] Division of Respiratory Medicine, University of British Columbia, Vancouver, British Columbia, Canada; [5] Department of Respiratory Medicine, Shiga University of Medical Science, Otsu, Shiga, Japan; [6] Cancer Imaging Department, British Columbia Cancer Agency, University of British Columbia, Vancouver, British Columbia, Canada

Correspondence to:
Dr H O Coxson, Department of Radiology, Vancouver General Hospital, 855 West 12th Ave, Room 3350 JPN, Vancouver, British Columbia, V5Z 1M9, Canada; harvey.coxson@vch.ca

Received 11 December 2008
Accepted 29 July 2009
Published Online First
2 September 2009

ABSTRACT

Background: A study was undertaken to determine if quantitative CT estimates of lung parenchymal over-inflation and airway dimensions in smokers with a normal forced expiratory volume in 1 s (FEV_1) can predict the rapid decline in FEV_1 that leads to chronic obstructive pulmonary disease (COPD).

Methods: Study participants (n = 143; age 45–72 years; 54% male) were part of a lung cancer screening trial, had a smoking history of >30 pack years and a normal FEV_1 and FEV_1/forced vital capacity (FVC) at baseline (mean (SD) FEV_1 99.4 (12.8)%, range 80.2–140.7%; mean (SD) FEV_1/FVC 77.9 (4.4), range 70.0–88.0%). An inspiratory multislice CT scan was acquired for each subject at baseline. Custom software was used to measure airway lumen and wall dimensions; the percentage of the lung inflated beyond a predicted maximal lung inflation, the low attenuation lung area with an *x* ray attenuation lower than −950 HU and the size distribution of the overinflated lung areas and the low attenuation area were described using a cluster analysis. Multiple regression analysis was used to test the hypothesis that these CT measurements combined with other baseline characteristics might identify those who would develop an excessive annual decline in FEV_1.

Results: The mean (SD) annual change in FEV_1 was −2.3 (4.7)% predicted (range −23.0% to +8.3%). Multiple regression analysis revealed that the annual change in FEV_1%predicted was significantly associated with baseline percentage overinflated lung area measured on quantitative CT, FEV_1%predicted, FEV_1/FVC and gender.

Conclusion: Quantitative CT scan evidence of over-inflation of the lung predicts a rapid annual decline in FEV_1 in smokers with normal FEV_1.

Chronic obstructive pulmonary disease (COPD) is an inflammatory lung disease caused by the inhalation of toxic particles and gases that results in destruction of the lung parenchyma and remodelling of the small airways.[1] Tobacco smoking is the most important risk factor for COPD, but the fact that only a minority of smokers develop COPD strongly suggests that the host response is equally important in the pathogenesis of this condition.[2 3]

That only a susceptible minority of smokers develop COPD was discovered in a classic study of the natural history of chronic bronchitis and emphysema by Fletcher *et al*.[2] This study showed that, over 8 years of follow-up, only 13% of participants experienced a decline in forced expiratory volume in 1 s (FEV_1) and therefore ended with a final FEV_1 that was low enough to satisfy the current diagnostic criteria for COPD.[2] Although recent data suggest that this small fraction may have been an underestimate, the concept that only a minority of heavy smokers develop COPD has not been challenged.[3] By the early 1970s it was recognised that the airflow limitation that defines COPD is caused by a combination of increased resistance in the small conducting airways and decreased parenchymal elasticity caused by emphysematous destruction.[4 5] Although many tests have been designed to detect small airway abnormalities at an early and hopefully reversible stage, they have been largely abandoned because they failed to identify the minority of smokers with normal expiratory flows who go on to develop COPD.[6 7]

The introduction of non-invasive quantitative imaging of both emphysematous lung destruction and airway remodelling has provided a fresh approach to detecting changes in the anatomy of the peripheral lung. Using these imaging approaches, investigators have shown that subjects with normal lung function may have emphysematous destruction in their lungs.[8 9] These observations led to the hypothesis that early emphysematous destruction might be associated with a subsequent rapid decline in FEV_1 that leads to COPD. The present study used computed tomography (CT) scans from subjects participating in a lung cancer screening study to quantify the inflation of the lung parenchyma, lung area with a lower *x* ray attenuation and airway dimensions, and correlated these measurements with serial spirometry that establish a subject's individual decline in FEV_1.

METHODS

Subjects

Subjects in the current study were from the British Columbia (BC) Cancer Agency lung cancer screening programme, the BC-Lung Health Cohort.[10] This sub-cohort is composed of smokers who had normal spirometry at baseline (ie, FEV_1 ⩾80% of predicted value; ratio of FEV_1 to forced vital capacity (FEV_1/FVC) ⩾70%); at least two spirometry measurements at least 6 months apart; and a baseline CT scan obtained using either a GE (GE Medical System, Milwaukee, Wisconsin, USA) or Siemens scanner (Siemens Medical Solutions; Erlangen, Germany).

Lung function

Spirometry was performed using American Thoracic Society guidelines without the administration of a bronchodilator.[11] FEV_1 was expressed as a percentage of the predicted value

(FEV_1%predicted) calculated using Crapo's equations.[12] FEV_1/FVC was calculated using actual values. The annual change in FEV_1%predicted (ΔFEV_1%predicted/year) was calculated for subjects with two visits as: (FEV_1%predicted at T1 − FEV_1%predicted at T0)/follow-up years. For subjects with more than two visits, ΔFEV_1%predicted/year was the slope of the regression line, in which all the available FEV_1%predicted measurements were plotted against age. A negative value of ΔFEV_1%predicted/year indicates worsening of the lung function.

CT technique

All CT scans were acquired in the volume scan mode at suspended full inspiration with the subject in the supine position. No intravenous contrast media were used. These CT scans were acquired using a GE scanner (Lightspeed Ultra, 120 kVp, 160 mAs, 1.25 mm slice thickness, standard reconstruction kernel) in 36 cases (25%) and using a Siemens scanner (Sensation 16, 120 kVp, 125 mAs, 1.0 mm slice thickness, B35f reconstruction kernel) in 107 cases (75%). These two image acquisition protocols have been shown to provide comparable CT densitometry measurements.[13]

Quantitative CT analysis

A quantitative analysis of the lung parenchyma was performed using custom software (EmphylxJ) as previously described.[13] Briefly, the lung parenchyma was segmented from the chest wall and large central blood vessels in all CT images using a modified border tracing algorithm with a prior position knowledge algorithm. Total lung volume was calculated by summing the segmented pixel area in each slice and multiplying by the slice thickness. For each pixel, the mean CT attenuation (in Hounsfield Units, HU) was calculated and converted to density (g/ml) by adding 1000 to the HU number and dividing by 1000,[14] and the lung inflation (ie, volume of gas/g of tissue) was calculated according to equation 1:[15]

$$\frac{\text{ml(gas)}}{\text{g(tissue)}} = \textit{Specific volume}_{\textit{(tissue \& gas)}} - \textit{Specific volume}_{\textit{(tissue)}} \quad (1)$$

where specific volume is the inverse of density. The density of the lung (tissue and gas) was measured from the CT scan, and the density of gas-free tissue was assumed to be 1.065 g/ml and constant for all subjects.[16]

The predicted total lung capacity (TLC) was obtained using the following equations (equations 2a and 2b) from Crapo *et al*:[17]

Women: Predicted TLC (ml) = 59 × height (cm) − 4537 (2a)

Men: Predicted TLC (ml) = 79.5 × height (cm) + 3.2 × age (years) − 7333 (2b)

The predicted lung weight was obtained by first calculating the predicted body weight using an equation described by Devine[18] (equations 3a and 3b), and then substituting body weight into the prediction equation for lung weight modified from that originally provided by Shohl[19] (see online supplement) (equation 4).

Women: Predicted body weight (g) = 45500 + 905.5 × (height (cm) −152.4) (3a)

Men: Predicted body weight (g) = 50000 + 905.5 × (height (cm) −152.4) (3b)

Predicted lung weight (g) = 0.017 × ideal body weight (g) − 88.12 (g) (4)

Since TLC is the maximal volume of gas within the lung, dividing it by the predicted lung weight provides an indication of maximal lung inflation. Total overinflated lung volume was calculated by summing the pixel area with a lung inflation value greater than the predicted maximal lung inflation value in each slice and multiplying by the slice thickness. This overinflation volume was expressed as a percentage of the total lung volume (ie, %overinflation).

The "upper lung zone" was defined as the region above the carina and zonal predominance was calculated using equation 5:

$$\text{zonal predominance} = \frac{\text{upper overinflation (\% of total upper lung)}}{\text{lower overinflation (\% of total lower lung)}} \quad (5)$$

The distribution was considered "upper zone predominant" if the result of equation 5 was >1 and was considered "diffuse" or "lower zone predominant" if it was ⩽1. A cluster analysis was used to estimate the size distribution of the overinflated areas.[9] The inverse slope of the log-log relationship of the size of the clusters (number of contiguous voxels that are inflated beyond the predicted value for maximum lung inflation for that individual) versus the number of clusters of that size is the power-law exponent (D). Individuals with diffuse small clusters of overinflated lung will have a steeper slope (ie, greater D) than individuals with larger overinflated regions. The low attenuation lung area (LAA) with an *x* ray attenuation lower than −950 HU (%LAA(−950)) was calculated using the standard threshold approach and used to estimate "emphysema".[20] The zonal predominance and D were also calculated for %LAA(−950).

Airway wall dimensions were measured for all visible airways cut in cross section on each CT image using the "full-width at half-maximum method".[21] Airway dimensions included lumen area (Ai), lumen perimeter (Pi), airway wall area (Aaw) and wall area expressed as the percentage of the total airway area ((Aaw/Aaw + Ai) = WA%) and a normalised airway wall estimate: square root of Aaw at Pi of 10 mm (ie, $\sqrt{}$Aaw at Pi10) (see online supplement).[22] A mean (SD) of 33.2 (3.1) airways were measured per subject.

Statistical analysis

Statistical analyses were performed using JMP software Version 7.0.1 (SAS Institute, Cary, North Carolina, USA). The primary outcome was ΔFEV_1%predicted/year and the explanatory variables were CT measurements of (1) overinflated lung (ie, %overinflation, zonal predominance and cluster analysis); (2) emphysema (ie, %LAA (−950 HU), zonal predominance and cluster analysis); and (3) airway dimensions (ie, Ai, %WA and $\sqrt{}$Aaw at Pi10). Covariates included age, sex, body mass index (BMI), current smoking status (ie, current or ex-smoker), pack years and baseline spirometry measurements (FEV_1%predicted and FEV_1/FVC). Three multivariate models were used to identify the CT variables associated with the primary outcome after adjusting for the covariates (overinflation, emphysema and airway dimensions were tested respectively in models 1, 2 and 3).

To illustrate the relationship between ΔFEV_1%predicted/year and baseline %overinflation, we divided the 143 subjects into quartiles according to baseline %overinflation (quartile 1 had the least %overinflation) and compared ΔFEV_1%predicted/year across four quartiles using the Wilcoxon test. A linear mixed effects model was used to evaluate the annual decline in FEV_1 (ml/year) for two groups (quartiles 1/2 and quartiles 3/4).[23] Data were expressed as mean (SD) and $p<0.05$ was considered significant.

RESULTS

Baseline characteristics

Descriptive characteristics of 143 subjects are shown in table 1 and baseline quantitative CT assessments are summarised in table 2.

Follow-up measurements of FEV_1

Seventy-two of 143 subjects (50.3%) were seen twice over 2.3 (0.8) years, 49 (34.3%) were seen three times over 2.3 (1.1) years and 22 (15.4%) were seen more than three times over 3.3 (1.4) years. The mean (SD) number of follow-up visits was 2.7 (0.8) (range 2–5) over 2.5 (1.1) years (range 0.5–6.4). ΔFEV_1%predicted/year observed over this time period averaged −2.3 (4.7)%/year (range −23.0 to +8.3%/year).

Risk factors associated with annual change in FEV_1%predicted

Table 3 shows the three multivariate models testing the association between CT measurements and ΔFEV_1%predicted/year. In model 1, %overinflation was inversely associated with ΔFEV_1%predicted/year whereas neither emphysema nor airway dimensions were associated with ΔFEV_1%predicted/year in models 2 and 3. In addition, in model 1, sex and baseline spirometry measurements were also associated with ΔFEV_1%predicted/year (male sex: −0.73, 95% CI −1.43 to −0.03, p = 0.04; FEV_1%predicted: −0.16, 95% CI −0.11 to −0.22, p<0.01; FEV_1/FVC: 0.19, 95% CI 0.36 to 0.01, p = 0.03).

Overinflation and annual change in FEV_1%predicted

There was a significant linear relationship between CT %overinflation and ΔFEV_1%predicted/year (see online supplement). The mean (SD) baseline %overinflation for quartiles 1–4 were 37.1 (1.5)%, 52.6 (0.8)%, 67.0 (1.1)% and 77.2 (0.6)%, respectively. The corresponding values of ΔFEV_1%predicted/year were −0.9 (0.6)%, −2.0 (0.7)%, −2.3 (0.7)% and −3.9 (1.0)%, and differed between quartiles 1/2 and 3/4 (p = 0.018, fig 1).

The mean annual decline in FEV_1 was 0.047 l/year and 0.068 l/year for quartile 1/2 and quartile 3/4 from the linear mixed effect model (quartile 1/2: FEV_1 (l) = 5.220 − 0.047 × age (years); quartile 3/4: FEV_1 (l) = 6.25 − 0.068 × age (years)). The FEV_1 at age 45, 50, 55, 60, 65, 70 and 75 years was calculated using these equations for quartile 1/2 and quartile 3/4 and the values were superimposed onto the figure of Fletcher *et al*[2] (fig 2).

DISCUSSION

The present results show a quantitative CT-based estimate of %overinflation using individual predicted maximal lung inflation is an independent predictor of rapid decline in lung function in smokers with normal baseline spirometry. The group with greater %overinflation at baseline exhibited a rate of decline in FEV_1 beyond the normal values predicted by Fletcher *et al*.[2] These results suggest that, when the FEV_1 is normal, a quantitative structural assessment by CT can distinguish the smokers who will develop COPD from those who will not.

In the current study we used standard prediction equations for TLC and a prediction equation for lung weight to estimate maximal normal lung inflation for each individual. The mean (SD) value of predicted maximal normal inflation of the whole group was 5.9 (0.2) ml/g (range 5.3–6.5), of which the corresponding HU was −830 (5.3) (range −846 to −811), which is substantially different from the fixed cut-off value of

Table 1 Baseline characteristics of study population

	Mean (SD)	Range
Sex (F/M)	66/77	
Age (years)	59.5 (6.4)	44.6–72.9
Height (cm)	171.5 (9.8)	149.9–195.6
Weight (kg)	81.6 (14.7)	52.2–122.6
BMI (kg/cm²)	27.7 (3.8)	18.7–37.5
Smoking (pack years)		
Current smokers (n = 38)	41.5 (11.4)	30–90
Ex-smokers (n = 105)	49.3 (21.0)	30–172
Lung function		
FEV_1 actual (l)	3.2 (0.8)	1.8–5.7
FEV_1%predicted (%)	99.4 (12.8)	80.2–140.7
FEV_1/FVC (%)	77.9 (4.4)	70.0–88.0

BMI, body mass index; FEV_1, forced expiratory flow in 1 s; FEV_1%predicted (%), (FEV_1/predicted FEV_1) × 100%; FVC, forced vital capacity; FEV_1/FVC (%), (FEV_1/FVC) × 100%.

Table 2 Characteristics of baseline quantitative CT assessments of subjects

	Mean (SD)	Range
Total lung volume(ml)	5086.2 (1350.3)	2608.1–9861.1
Mean lung density (g/ml)	0.2 (0.0)	0.1–0.2
Lung overinflation		
%overinflation	58.4 (16.4)	15.9–83.7
Cluster analysis	1.5 (0.2)	1.2–2.1
Upper zone predominant	n = 102	
Diffuse distribution	n = 7	
Lower zone predominant	n = 34	
Emphysema		
%LAA(−950 HU)	2.9 (2.6)	0.2–13.3
Cluster analysis	3.1 (0.4)	2.1–4.4
Upper zone predominant	n = 35	
Diffuse distribution	n = 10	
Lower zone predominant	n = 98	
Airway dimensions		
Lumen area, Ai (mm²)	6.8 (2.3)	2.1–15.1
WA %	76.8 (3.5)	67.5–84.9
√Aaw at Pi10 (mm)	4.4 (0.2)	3.9–5.1

Aaw, airway wall area; Ai, lumen area; LAA, low attenuation lung area; Pi, lumen perimeter; WA %, wall area expressed as the percentage of the total airway area. %overinflation, (volume of overinflated lung/volume of total lung) × 100%; %LAA (−950 HU), (volume of lung areas with *x* ray attenuation lower than −950 HU/volume of total lung) × 100%; WA%, (airway wall area/(airway wall area + lumen area)) × 100%; √Aaw at Pi10 (mm), √Aaw for a standardised airway with an internal perimeter (ie, Pi) of 10 mm.

Table 3 Multivariate models testing the association between the quantitative CT measurements and annual change in FEV_1%predicted

	Estimate (95% CI)	p Value
Model 1*: Lung overinflation		
%overinflation	−0.04 (−0.08 to −0.02)	0.04
Cluster analysis	−0.49 (−11.34 to 10.35)	0.93
Upper zone predominant	0.02 (−0.10 to 0.14)	0.74
Model 2*: Emphysema		
%LAA (−950 HU)	−0.13 (−0.47 to 0.21)	0.46
Cluster analysis	−0.61 (−2.68 to 1.45)	0.56
Upper zone predominant	0.11 (−1.38 to 1.59)	0.89
Model 3*: Airway dimensions		
Ai (mm²)	0.17 (−0.40 to 0.73)	0.56
WA %	0.00 (−0.53 to 0.53)	0.99
√Aaw at Pi10 (mm)	1.4 (−4.45 to 7.25)	0.64

*Models were adjusted for sex, age, body mass index, smoking status, pack years, FEV_1%predicted and FEV_1/FVC at baseline.
Aaw, airway wall area; Ai, lumen area; LAA, low attenuation lung area; Pi, lumen perimeter; WA %, wall area expressed as the percentage of the total airway area. %overinflation, (volume of overinflated lung/volume of total lung) × 100%; %LAA (−950 HU), (volume of lung areas with *x* ray attenuation lower than −950 HU/volume of total lung) × 100%; WA %, (airway wall area/(airway wall area + lumen area)) × 100%; √Aaw at Pi10 (mm), √Aaw for a standardised airway with an internal perimeter (Pi) of 10 mm.

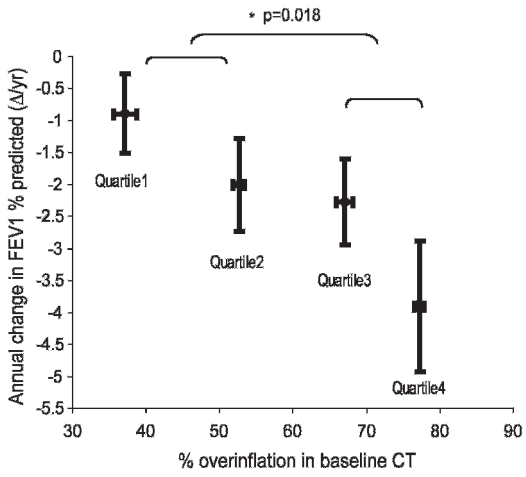

Figure 1 Comparison of annual change in percentage predicted forced expiratory volume in 1 s (ΔFEV_1%predicted/year) across the four quartiles of baseline CT overinflation volume expressed as a percentage of the total lung volume (%overinflation). Mean (SD) baseline %overinflation was 37.1 (1.5)%, 52.6 (0.8)%, 67.0 (1.1)% 77.2 (0.6)% for quartiles 1–4, respectively. Mean (SD) ΔFEV_1%predicted/year was −0.9 (0.6)%/year, −2.0 (0.7)%/year, −2.3 (0.7)%/year and −3.9 (1.0)%/year, respectively, and differed between quartiles 3/4 and 1/2 ($p = 0.018$).

−950 HU that is commonly used to define emphysema on CT scanning.[20] Importantly, we do not claim that the minimally overinflated tissue identified by this procedure has undergone emphysematous destruction because we have no direct histological evidence. Based on pathology data, Leopold and Gough[24] and McLean[25] concluded that the dilation and destruction of the respiratory bronchioles that define centrilobular emphysema, the most common form of emphysema in smokers, is preceded by the disease in the terminal and preterminal bronchioles. We therefore strongly suspect that the minimal overinflation observed in this study may be caused by either minimal loss in the elastic recoil properties of the gas exchanging tissue and/or an increased resistance in terminal conducting airways due to inflammatory and tissue remodelling processes, both of which can occur before true emphysematous destruction.

The significance of the "overinflation" raised in our study is in agreement with that of the "hyperinflation" described by other investigators.[26 27] Hyperinflation results from increased lung compliance due to emphysema and expiratory flow limitation, and patients may not perceive the negative results of it until an advanced stage because it develops slowly and insidiously over years.[28] Ofir *et al*[27] examined "hyperinflation" using lung function tests (total lung capacity, residual volume and functional residual volume) in patients with COPD GOLD stage I and healthy subjects. They found that patients with GOLD stage I COPD had more hyperinflation which increased as the intensity of dyspnoea increased. Casanova *et al*[26] found that hyperinflation, independent of the BODE index, predicted mortality over a follow-up period of 34 months in 689 subjects with COPD. Although the findings that we have obtained with imaging tools are compatible with these studies of hyperinflation, further investigation is required to examine the relationship between these two measures of early disease.

Only a few studies have examined the relationship between quantitative CT measurements of the lung parenchyma and decline in lung function. Remy-Jardin *et al*[29] examined 111 smokers and non-smokers and reported that subjects with emphysema visualised by radiologists at baseline had a more rapid decline in lung function than did those with normal CT scans. On the other hand, Parr *et al*[30] and Stolk *et al*[31] found no relationship between baseline CT emphysema and the subsequent decline in FEV_1 in subjects with COPD. These studies recruited many subjects who already had moderate COPD at

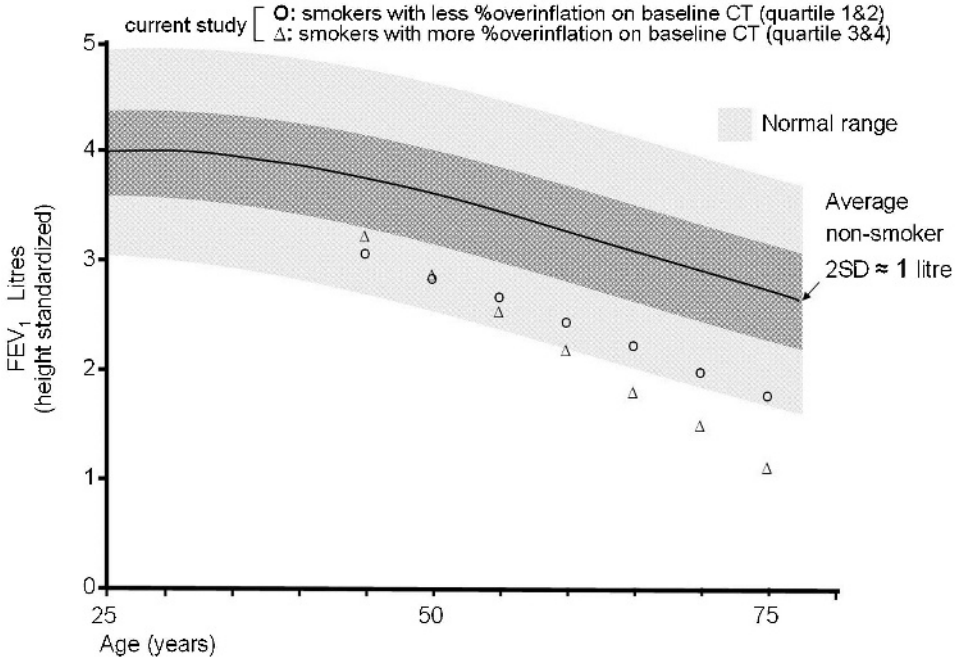

Figure 2 The line with surrounding grey band is the "normal range" (ie, mean ± 2SD) of forced expiratory volume in 1 s (FEV_1 in litres) observed in non-smokers by Fletcher *et al*.[2] Open circles and triangles represent an extrapolation of the data from the current study. Open circles are data from quartile 1/2, in which smokers had less overinflation volume expressed as a percentage of the total lung volume (%overinflation) at baseline and an annual decline in FEV_1 of 0.047 l. Triangles are data from quartile 3/4, in which smokers had more %overinflation at baseline and an annual decline in FEV_1 of 0.068 l.

baseline, which contrasts sharply with the present study which was specifically designed to determine whether CT might identify those smokers who had normal initial spirometry and subsequently developed COPD.

In contrast to the extent of overinflation, the size and location of the overinflated regions, as assessed by cluster analysis and zonal predominance, was less helpful in identifying "susceptible smokers". Moreover, although Nakano *et al*[22] showed that CT measurements of thickening and narrowing of the relatively large airways serve as a surrogate for the pathological changes in the small airways that are not measurable on CT scans, we failed to identify a relationship between the CT airway dimensions and ΔFEV_1%predicted. There are several possible reasons for this observation. Most important, the differences in airway dimensions that accompany a relatively small change in lung function are probably beyond the resolution of CT scans. Although many investigators have shown relationships between airway wall dimensions and airflow obstruction in cross-sectional studies, the range of lung function in those studies was much larger than in the present study.[21] Second, quantitative histological studies have shown that statistically significant airway wall thickening does not become apparent until the later stages of disease (GOLD stages III and IV) with an FEV_1%predicted <50.[32] Finally, our method for measuring airway dimensions may not be optimal for assessing subtle changes. Hasegawa *et al*[33] used volumetric scanning to show that airflow limitation in COPD is more closely related to the dimensions of the distal smaller airways (ie, 5th and 6th generations) than those of proximal larger airways (ie, 3rd and 4th generations).

Fletcher *et al*[2] were the first to show a relationship between the initial FEV_1 and its subsequent decline and referred to the phenomenon as the "horse racing" effect. However, Burrows *et al*[34] observed an opposite relationship between ΔFEV_1 and initial FEV_1, such that the higher the initial FEV_1, the more negative the ΔFEV_1. They pointed out that this was due to "regression toward the mean", a phenomenon in which subjects performing especially well on their first test show a greater decline because of a poorer performance on subsequent tests. Burrows and Stanescu[6 34] also observed an association between initial FEV_1/FVC and ΔFEV_1%predicted, and suggested that FEV_1/FVC might provide a more reliable indicator of future loss in FEV_1. Our results confirm the findings of Burrows and Stanescu and extend their observations by showing that CT evidence of lung parenchymal overinflation is an independent predictor of decline in FEV_1.

Although the lack of an association between smoking intensity (ie, pack years) and decline in lung function might be a little surprising, this is consistent with other reports in the literature.[35] We also think this lack of association between pack years and the decline in FEV_1 supports Fletcher's concept that "non-susceptible smokers" remain unaffected regardless of their smoking history. The converse is also true—that "susceptible smokers" exhibit a decline in lung function independent of their smoking status.

A limitation of this study is that it was not originally designed as a study of COPD but was added on to a lung cancer screening cohort. Subjects were therefore not randomly chosen from the population. Follow-up spirometry was arranged at the time of follow-up CT scans which depended on the characteristics of the lung nodule(s) found on the initial CT scan. This means that different numbers of spirometric tests were performed at different frequencies between subjects. To overcome this limitation we used ΔFEV_1%predicted/year to normalise the difference in the follow-up period and the number of sampling points among subjects. ΔFEV_1%predicted/year also adjusted for the normal annual loss due to ageing and corrected for differences between women and men.

In summary, we conclude that the quantitative assessment of the lung inflated beyond individually predicted maximal lung inflation on initial CT scans may be able to identify the "susceptible minority of smokers" who eventually will develop COPD. Our working hypothesis is that the minimally overinflated lung contains the earliest forms of lesions that either increase peripheral airway resistance and/or increase lung compliance by initiating emphysematous destruction.

Acknowledgements: The authors thank Anh-Toan Tran and Ida Chan for technical assistance in developing the lung analysis application and Xuekui Zhang for statistical suggestions.

Authors' contributions: All authors contributed to the design of the study and the drafting and revising of the manuscript. RY, YN and JCW performed the laboratory work and statistical analysis. JCH, PDP, HOC, DDS and SL are the principal investigators of the project, obtained funding for and supervised the project. SL and AMM initially recruited the subjects and DDS provided statistical suggestions. All authors read and approved the final manuscript.

Funding: HOC is a Canadian Institutes of Health Research/British Columbia Lung Association New Investigator and is also supported in part by the University of Pittsburgh COPD SCCOR NIH 1P50 HL084948 and R01 HL085096 from the National Heart, Lung and Blood Institute, National Institutes of Health, Bethesda, MD to the University of Pittsburgh. PDP is a MSFHR Distinguished scholar and the Jacob Churg Distinguished Researcher. DDS is a Canada Research Chair in COPD and a Senior Scholar with the Michael Smith Foundation for Health Research. SL is supported by NIH grant 1PO1-CA96964, U01CA96109 and NCI contract N01-CN-85188. This project was funded by a CIHR Industry partnership grant with GlaxoSmithKline.

Competing interests: JCH has served as a consultant, given lectures and participated in advisory boards of several major pharmaceutical companies in the past five years. The total reimbursement for these activities is less than $20 000. PDP was the principal investigator of a Merck Frosst supported research programme to investigate gene expression in the lungs of patients who have COPD. He and collaborators have received approximately $200 000 for this project. These funds have supported the technical personnel and expendables involved in the project. He sits on an advisory board for Talecris Biotherapeutics who make anti-one antitrypsin replacement therapy. He is the principal investigator of a project funded by GlaxoSmithKline to develop CT-based algorithms to quantify emphysema and airway disease in COPD. With collaborators he has received approximately $300 000 to develop and validate these techniques. These funds have been applied solely to the research to support programmers and technicians. DDS has received research funding from GlaxoSmithKline and AstraZeneca for projects on chronic obstruction pulmonary disease. He has also received honoraria for speaking engagements for talks on COPD sponsored by these organizations. HOC received $11 000 in 2005 and $4800 in 2006 and 2007 for serving on an advisory board for GlaxoSmithKline. He is the co-investigator on two multicentre studies sponsored by GlaxoSmithKline and has received travel expenses to attend meetings related to the project. He has three contract service agreements with GlaxoSmithKline to quantify the CT scans in subjects with COPD and a service agreement with Spiration Inc to measure changes in lung volume in subjects with severe emphysema. A percentage of HOC's salary between 2003 and 2006 (15 000 US $/year) derives from contract funds provided to a colleague PDP by GlaxoSmithKline for the development of validated methods to measure emphysema and airway disease using computed tomography. HOC is the co-investigator (with DDS) on a Canadian Institutes of Health-Industry (Wyeth) partnership grant. There is no financial relationship between any industry and the current study. RY, JCW, YN, SL and AMMcW have no competing interests in the content of this paper.

Ethics approval: The University of British Columbia Clinical Ethics Review board approved the study and all subjects provided informed written consent for the use of all materials and data.

Provenance and peer review: Not commissioned; externally peer reviewed.

REFERENCES

1. **Burrows B,** Knudson RJ, Cline MG, *et al*. Quantitative relationships between cigarette smoking and ventilatory function. *Am Rev Respir Dis* 1977;**115**:195–205.
2. **Fletcher CM.** Letter: Natural history of chronic bronchitis. *BMJ* 1976;**1**:1592–3.
3. **Rennard SI,** Vestbo J. COPD: the dangerous underestimate of 15%. *Lancet* 2006;**367**:1216–9.
4. **Hogg JC,** Macklem PT, Thurlbeck WM. Site and nature of airway obstruction in chronic obstructive lung disease. *N Engl J Med* 1968;**278**:1355–60.
5. **Macklem PT,** Mead J. Resistance of central and peripheral airways measured by a retrograde catheter. *J Appl Physiol* 1967;**22**:395–401.

6. **Stanescu D,** Sanna A, Veriter C, *et al*. Identification of smokers susceptible to development of chronic airflow limitation: a 13-year follow-up. *Chest* 1998;**114**:416–25.
7. **Vestbo J,** Hogg JC. Convergence of the epidemiology and pathology of COPD. *Thorax* 2006;**61**:86–8.
8. **Gevenois PA,** Scillia P, de Maertelaer V, *et al*. The effects of age, sex, lung size, and hyperinflation on CT lung densitometry. *AJR Am J Roentgenol* 1996;**167**:1169–73.
9. **Mishima M,** Hirai T, Itoh H, *et al*. Complexity of terminal airspace geometry assessed by lung computed tomography in normal subjects and patients with chronic obstructive pulmonary disease. *Proc Natl Acad Sci U S A* 1999;**96**:8829–34.
10. **McWilliams A,** Mayo J, MacDonald S, *et al*. Lung cancer screening: a different paradigm. *Am J Respir Crit Care Med* 2003;**168**:1167–73.
11. **American Thoracic Society**. Standardization of Spirometry, 1994 update. *Am J Respir Crit Care Med* 1995;**152**:1107–36.
12. **Crapo RO,** Morris AH, Gardner RM. Reference spirometric values using techniques and equipment that meet ATS recommendations. *Am Rev Respir Dis* 1981;**123**:659–64.
13. **Yuan R,** Mayo JR, Hogg JC, *et al*. The effects of radiation dose and CT manufacturer on measurements of lung densitometry. *Chest* 2007;**132**:617–23.
14. **Hedlund LW,** Vock P, Effmann EL. Computed tomography of the lung. Densitometric studies. *Radiol Clin North Am* 1983;**21**:775–88.
15. **Coxson HO,** Mayo JR, Behzad H, *et al*. Measurement of lung expansion with computed tomography and comparison with quantitative histology. *J Appl Physiol* 1995;**79**:1525–30.
16. **Hogg JC,** Nepszy S. Regional lung volume and pleural pressure gradient estimated from lung density in dogs. *J Appl Physiol* 1969;**27**:198–203.
17. **Crapo RO,** Morris AH, Clayton PD, *et al*. Lung volumes in healthy nonsmoking adults. *Bull Eur Physiopathol Respir* 1982;**18**:419–25.
18. **Devine BJ.** Gentamicin therapy. *Drug Intell Clin Pharm* 1974;**8**:650–5.
19. **Shohl AT.** *Mineral metabolism*. New York: Reinhold Publishing Corporation, 1939.
20. **Gevenois PA,** De Vuyst P, de Maertelaer V, *et al*. Comparison of computed density and microscopic morphometry in pulmonary emphysema. *Am J Respir Crit Care Med* 1996;**154**:187–92.
21. **Nakano Y,** Muro S, Sakai H, *et al*. Computed tomographic measurements of airway dimensions and emphysema in smokers. Correlation with lung function. *Am J Respir Crit Care Med* 2000 Sep;**162**(3 Pt 1):1102–8.
22. **Nakano Y,** Wong JC, de Jong PA, *et al*. The prediction of small airway dimensions using computed tomography. *Am J Respir Crit Care Med* 2005;**171**:142–6.
23. **Feldman HA.** Families of lines: random effects in linear regression analysis. *J Appl Physiol* 1988;**64**:1721–32.
24. **Leopold JG,** Gough J. The centrilobular form of hypertrophic emphysema and its relation to chronic bronchitis. *Thorax* 1957;**12**:219–35.
25. **McLean KH.** The histology of localized emphysema. *Australas Ann Med* 1957;**6**:282–94.
26. **Casanova C,** Cote C, de Torres JP, *et al*. Inspiratory-to-total lung capacity ratio predicts mortality in patients with chronic obstructive pulmonary disease. *Am J Respir Crit Care Med* 2005;**171**:591–7.
27. **Ofir D,** Laveneziana P, Webb KA, *et al*. Mechanisms of dyspnea during cycle exercise in symptomatic patients with GOLD stage I chronic obstructive pulmonary disease. *Am J Respir Crit Care Med* 2008;**177**:622–9.
28. **O'Donnell DE.** Hyperinflation, dyspnea, and exercise intolerance in chronic obstructive pulmonary disease. *Proc Am Thorac Soc* 2006;**3**:180–4.
29. **Remy-Jardin M,** Edme JL, Boulenguez C, *et al*. Longitudinal follow-up study of smoker's lung with thin-section CT in correlation with pulmonary function tests. *Radiology* 2002;**222**:261–70.
30. **Parr DG,** White AJ, Bayley DL, *et al*. Inflammation in sputum relates to progression of disease in subjects with COPD: a prospective descriptive study. *Respir Res* 2006;**7**:136.
31. **Stolk J,** Putter H, Bakker EM, *et al*. Progression parameters for emphysema: a clinical investigation. *Respir Med* 2007;**101**:1924–30.
32. **Hogg JC,** Chu F, Utokaparch S, *et al*. The nature of small-airway obstruction in chronic obstructive pulmonary disease. *N Engl J Med* 2004;**350**:2645–53.
33. **Hasegawa M,** Nasuhara Y, Onodera Y, *et al*. Airflow limitation and airway dimensions in chronic obstructive pulmonary disease. *Am J Respir Crit Care Med* 2006;**173**:1309–15.
34. **Burrows B,** Knudson RJ, Camilli AE, *et al*. The "horse-racing effect" and predicting decline in forced expiratory volume in one second from screening spirometry. *Am Rev Respir Dis* 1987;**135**:788–93.
35. **Celli BR,** Cote CG, Marin JM, *et al*. The body-mass index, airflow obstruction, dyspnea, and exercise capacity index in chronic obstructive pulmonary disease. *N Engl J Med* 2004;**350**:1005–12.

Lung alert

The *sst1* locus controls granuloma necrosis in tuberculosis

There is broad variation in susceptibility to *Mycobacterium tuberculosis* (MTB), and mouse models play a key role in elucidating the underlying mechanisms. The authors tested the hypothesis that caseation within pulmonary lesions is a specific effect of the *sst1* (supersusceptibility to tuberculosis 1) locus on chromosome 1.

Typical mouse lesions described in the literature lack central caseation. However, the C3HeB/FeJ strain of mouse develops large necrotising granulomas after exposure to MTB. The authors compared the course of infection in an MTB-resistant mouse strain (B6) with an *sst1*-susceptible congenic strain (B6.C3H-*sst1*) which was genetically identical except for the interval containing the *sst1* locus.

They found that, although initial dissemination was similar, bacterial loads, clinical disease, lung necrosis and mortality were considerably worse in the strain containing the *sst1*-susceptible allele. In addition, relapse after 3 months of isoniazid was faster and more rampant in this group. After demonstrating significantly slower disease progression and milder histopathology in the B6.C3H-*sst1* strain compared with the C3HeB/FeJ strain, the authors concluded that the effect of the *sst1* locus is modified by the genetic background of the host. Enhanced pro-inflammatory cytokine production by macrophages was observed in the susceptible strains; however, this appears to be controlled by loci other than *sst1*.

Further characterisation of *sst1*-encoded molecular mechanisms may not only shed light on a key aspect of the pathogenesis of tuberculosis, but may also suggest therapeutic interventions to reduce lung pathology and transmission of the pathogen.

► Pichugin AV, Yan B, Sloutsky A, *et al*. Dominant role of the sst1 locus in pathogenesis of necrotizing lung granulomas during chronic tuberculosis infection and reactivation in genetically resistant hosts. *Am J Pathol* 2009;**174**:2190–201

M Almond

Correspondence to: Dr M Almond, ST1 Oncology, Royal Marsden Hospital, London, UK; mhalmond@gmail.com

Provenance and peer review: Commissioned; not externally peer reviewed.

Thorax 2009;**64**:949. doi:10.1136/thx.2009.122879